

## Dielectric Constants of Zr Silicates: A First-Principles Study

G.-M. Rignanese, F. Detraux, and X. Gonze

*Unité de Physico-Chimie et de Physique des Matériaux, Université Catholique de Louvain,  
1 Place Croix du Sud, B-1348 Louvain-la-Neuve, Belgium*

*Research Center on Microscopic and Nanoscopic Materials and Electronic Devices (CERMIN), Université Catholique de Louvain,  
B-1348 Louvain-la-Neuve, Belgium*

Angelo Bongiorno and Alfredo Pasquarello

*Institut de Théorie des Phénomènes Physiques (ITP), Ecole Polytechnique Fédérale de Lausanne (EPFL),  
CH-1015 Lausanne, Switzerland*

*Institut Romand de Recherche Numérique en Physique des Matériaux (IRRMA), CH-1015 Lausanne, Switzerland  
(Received 14 January 2002; published 26 August 2002)*

Using density-functional theory, we compute the optical and static dielectric constants for a set of Zr silicates modeled by various  $\text{SiO}_2$  crystals, with Zr atoms substitutional to Si, and by an amorphous structure. We then derive a microscopic scheme that relates the dielectric constants to structural units centered on Si and Zr atoms through the definition of characteristic parameters. Applied to amorphous  $(\text{ZrO}_2)_x(\text{SiO}_2)_{1-x}$ , these schemes describe the observed dependence of the dielectric constants on the Zr concentration and highlight the role of  $\text{ZrO}_6$  units.

DOI: 10.1103/PhysRevLett.89.117601

PACS numbers: 77.22.-d, 61.43.-j, 63.50.+x

Feature size reduction has governed the research in electronic devices for over four decades [1,2]. The dominant technology based on  $\text{SiO}_2$  as gate dielectric is now approaching fundamental limits. Scaled device operation requires higher gate capacitances, but further thinning of the oxide layer is precluded by severe leakage problems. Current research is therefore focusing on the replacement of  $\text{SiO}_2$  by materials with higher permittivity (high- $\epsilon$ ).

Zr silicates appear at this time as the most promising candidates for next-generation gate dielectrics [3]. Amorphous films are stable in contact with Si up to high temperature, preventing the formation of undesired low- $\epsilon$  interfacial layers. The dielectric properties of these materials constitute an issue of great practical relevance. Early experimental measurements suggested a supralinear dependence of the static dielectric constant  $\epsilon_0$  on the Zr concentration [4]. While several phenomenological theories addressed this behavior [5,6], more recent data appear to favor instead a close to linear dependence [7,8].

In tackling this technological problem, we face the more general issue of predicting the dielectric properties of amorphous alloys from first principles. Brute force analysis of numerous large supercells is beyond present computational capabilities. To overcome this difficulty, we establish a relationship between the dielectric properties of Zr silicates and their underlying nanoscopic structure. Using density-functional theory (DFT), we compute optical and static dielectric constants for various model structures of Zr silicates, both ordered and disordered. We introduce a scheme which relates the dielectric constants to the local bonding of Si and Zr atoms. This scheme is based on the definition of parameters characteristic of the basic structural units (SUs) formed by Si and Zr atoms

and their nearest neighbors. Applied to amorphous Zr silicates, our scheme provides a good description of measured dielectric constants, both optical [8,9] and static [7,8], and reveals the important contribution of  $\text{ZrO}_6$  SUs to the static dielectric constant.

We consider model structures of  $(\text{ZrO}_2)_x(\text{SiO}_2)_{1-x}$ , nine crystalline and one amorphous, with  $x$  ranging from 0 to 0.5, and describe them in terms of cation-centered SUs. We start with three different  $\text{SiO}_2$  polymorphs ( $x = 0$ ):  $[\text{C}_0]$   $\alpha$ -cristobalite with four  $\text{SiO}_4$  SUs per unit cell,  $[\text{Q}_0]$   $\alpha$ -quartz with three  $\text{SiO}_4$  SUs, and  $[\text{S}_0]$  stishovite with two  $\text{SiO}_6$  SUs. By substituting one of the Si atoms by a Zr atom for each of these models, we generate three new crystal structures:  $[\text{C}_1]$   $\text{Zr}^{\text{Si}}$  in  $\alpha$ -cristobalite with three  $\text{SiO}_4$  and one  $\text{ZrO}_4$  SUs per unit cell ( $x = 0.25$ ),  $[\text{Q}_1]$   $\text{Zr}^{\text{Si}}$  in  $\alpha$ -quartz with two  $\text{SiO}_4$  and one  $\text{ZrO}_4$  SUs ( $x = 0.33$ ), and  $[\text{S}_1]$   $\text{Zr}^{\text{Si}}$  in stishovite with one  $\text{SiO}_6$  and one  $\text{ZrO}_6$  SUs. Then, starting from  $[\text{Z}_2]$  zircon which contains two  $\text{SiO}_4$  and two  $\text{ZrO}_8$  SUs per unit cell ( $x = 0.5$ ), we replace Zr by Si and generate two other structures:  $[\text{Z}_1]$   $\text{Si}^{\text{Zr}}$  in zircon with two  $\text{SiO}_4$ , one  $\text{SiO}_6$ , and one  $\text{ZrO}_8$  SUs ( $x = 0.25$ ), and  $[\text{Z}_0]$  fully Si-substituted zircon with two  $\text{SiO}_4$  and  $\text{SiO}_6$  SUs ( $x = 0$ ). Finally, the amorphous structure is generated using classical molecular dynamics with empirical potentials [10]. We use a periodically repeated cubic cell containing 3  $\text{ZrO}_4$  and 17  $\text{SiO}_4$  SUs ( $x = 0.15$ ) at a fixed density of  $3.12 \text{ g/cm}^3$ . Starting from random atomic positions, the melt is equilibrated at 5500 K for 250 ps. A quench with a cooling rate of  $\sim 10 \text{ K/ps}$  gives the final amorphous structure. We find that the Si atoms are all fourfold coordinated and that the Zr atoms show an average coordination of 6.3, in accord with experimental data [5,9]. In

this study, only a single disordered structure could be afforded because of the noticeable computational cost associated.

The atomic coordinates and the cell parameters of all our model structures are fully relaxed within the local density approximation (LDA) to DFT. The corresponding dynamical and dielectric properties are computed within a variational approach to density-functional perturbation theory, as implemented in the ABINIT package [11]. We refer to previous work on zircon for technical details [12]. The calculated optical and static dielectric constants [13] for our model structures are given in Table I. Because of the well-known limitations of the LDA, the theoretical values are larger than the experimental ones (when available) by about 10%.

In order to understand how the optical dielectric constant ( $\epsilon_\infty$ ) depends on the underlying atomic nanostructure, we consider the electronic polarizability  $\bar{\alpha}$  which is related to  $\epsilon_\infty$  by the Clausius-Mosotti relation [6,8]:

$$\frac{\epsilon_\infty - 1}{\epsilon_\infty + 2} = \frac{4\pi \bar{\alpha}}{3 \bar{V}}, \quad (1)$$

where  $\bar{V}$  is the average SU volume. The polarizability  $\bar{\alpha}$  can be taken as a local and additive quantity, in contrast with  $\epsilon_\infty$ . Therefore, we define  $\alpha_i$  values for each SU  $i$ , where  $i \equiv \text{SiO}_n$  (with  $n = 4$  or  $6$ ) or  $\text{ZrO}_n$  (with  $n = 4, 6$ , or  $8$ ), such that

$$\bar{\alpha} = \sum_i x_i \alpha_i, \quad (2)$$

where  $x_i$  is the molecular fraction. In Table II, we report the five  $\alpha_i$  values that we obtain by solving in a least square sense the overdetermined system based on the calculated  $\epsilon_\infty$  values for the nine crystalline models. The optical dielectric constants derived from these  $\alpha_i$  values using Eqs. (1) and (2) compare well with those calculated from first principles, showing average and maximal errors smaller than 1% and 2.5%, respectively.

TABLE I. Composition ( $x$ ), optical ( $\epsilon_\infty$ ) and static ( $\epsilon_0$ ) dielectric constants, volume ( $\bar{V}$ ) in bohr<sup>3</sup>, polarizability  $\bar{\alpha}$  in bohr<sup>3</sup>, characteristic dynamical charge ( $\bar{Z}$ ), and characteristic force constant ( $\bar{C}$ ) in hartree/bohr<sup>2</sup> for the various model systems.

Model	$x$	$\epsilon_\infty$	$\epsilon_0$	$\bar{V}$	$\bar{\alpha}$	$\bar{Z}$	$\bar{C}$
$C_0$	0.00	2.38	4.30	264.77	19.92	4.21	0.4391
$C_1$	0.25	2.76	5.25	273.21	24.12	4.59	0.3895
$Q_0$	0.00	2.54	4.83	240.34	19.46	4.28	0.4169
$Q_1$	0.33	2.91	5.84	275.28	25.56	4.85	0.3661
$S_0$	0.00	3.36	10.33	153.74	16.16	4.81	0.2716
$S_1$	0.50	4.44	24.20	201.88	25.74	6.14	0.1188
$Z_0$	0.00	3.37	10.11	167.80	17.68	4.76	0.2512
$Z_1$	0.25	3.94	18.36	189.74	22.42	5.29	0.1287
$Z_2$	0.50	4.13	11.81	213.28	26.00	5.58	0.2385
$A$	0.15	3.24	8.92	213.12	21.75	4.83	0.2424

For the amorphous model, which was not used to determine the  $\alpha_i$  values, the derived value  $\epsilon_\infty = 3.25$  is in excellent agreement with the first-principles result  $\epsilon_\infty = 3.24$ . These results justify *a posteriori* the use of Eqs. (1) and (2) to model the optical dielectric constant.

For the static dielectric constant ( $\epsilon_0$ ), the phonon contributions preclude a description in terms of a single local and additive quantity as the electronic polarizability. To overcome this difficulty, we focus on the difference between dielectric constants ( $\Delta\epsilon$ ):

$$\Delta\epsilon = \epsilon_0 - \epsilon_\infty = \frac{4\pi}{\Omega_0} \sum_m \frac{S_m}{\omega_m^2} = \frac{4\pi \bar{Z}^2}{\bar{V} \bar{C}}, \quad (3)$$

where  $\omega_m$  and  $S_m$  are the frequency and the oscillator strength of the  $m$ th mode. The volume of the primitive unit cell  $\Omega_0$  is related to the volume  $\bar{V}$  and to the number of SUs  $\bar{N}$  by  $\Omega_0 = \bar{N}\bar{V}$ . The characteristic dynamical charge  $\bar{Z}$  and characteristic force constant  $\bar{C}$  are defined by  $\bar{Z}^2 = (\sum_\kappa Z_\kappa^2)/\bar{N}$  and  $\bar{C}^{-1} = (\sum_m S_m/\omega_m^2)/\bar{N}$ , where  $Z_\kappa$  are the atomic Born effective charges.

Calculated values of the electrostatic force constant  $C_p = 4\pi\bar{Z}^2/\bar{V}$  and of  $\bar{C}$  for all our model structures are given in Fig. 1. In general,  $\Delta\epsilon$  is found to increase for a Si  $\rightarrow$  Zr substitution (subscripts: 0  $\rightarrow$  1, dashed lines). The increase in  $\Delta\epsilon$  results from the combination of two effects:  $\bar{C}$  decreases and  $C_p$  increases. Concerning  $\bar{C}$ , the Si  $\rightarrow$  Zr substitution leads to a decrease of the strength of the Zr-O bonds compared to Si-O bonds, and consequently to a lowering of the phonon frequencies. The increase of  $C_p$  upon a Si  $\rightarrow$  Zr substitution is related to the increase of  $\bar{Z}$  (Table I), though partially compensated by the concomitant increase of  $\bar{V}$ . For  $Z_0$ ,  $Z_1$ , and  $Z_2$ , this simple analysis does not apply because the considered substitutions also lead to changes of the atomic coordination.

For SUs with fourfold coordinated cations (Fig. 1, black and white symbols),  $C_p$  is lower than for those with sixfold or eightfold coordinated cations (gray symbols). Moreover, the higher  $C_p$ , the larger the variation of  $\Delta\epsilon$  associated with a Si  $\rightarrow$  Zr substitution. This is particularly true for sixfold coordinated atoms, for which  $\Delta\epsilon$  can be very large (see  $S_1$  and  $Z_1$ ). In fact, these configurations resemble those in  $\text{ABO}_3$  perovskites. The enhancement of  $\Delta\epsilon$  originates from very low frequency modes in which the cations (A or B) move in opposition

TABLE II. Polarizability ( $\alpha$  in bohr<sup>3</sup>), characteristic dynamical charge ( $Z$ ), and characteristic force constant ( $C$  in hartree/bohr<sup>2</sup>) of structural units.

	$\text{SiO}_4$	$\text{SiO}_6$	$\text{ZrO}_4$	$\text{ZrO}_6$	$\text{ZrO}_8$
$\alpha$	19.68	16.14	37.37	35.35	32.69
$Z$	4.29	4.92	5.66	7.16	6.73
$C$	0.3597	0.2176	0.4202	0.0817	0.1153

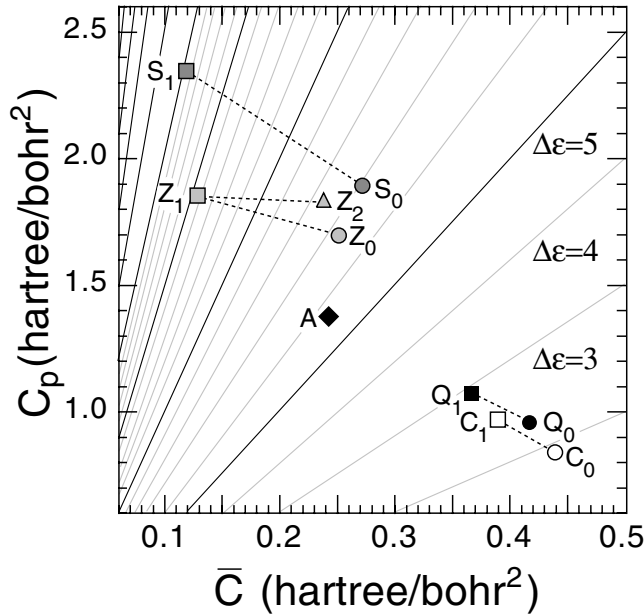


FIG. 1. Electrostatic force constant  $C_p$  vs characteristic force constant  $\bar{C}$  (expressed in hartree/bohr<sup>2</sup>) for the various model systems. The solid lines represent iso- $\Delta\epsilon$  starting at  $\Delta\epsilon = 2$  in the lower-right corner with strides of 1 and 5 between gray and black lines, respectively. The dashed lines relate model systems that differ by the substitution of one Si atom by a Zr atom (Si  $\rightarrow$  Zr).

with the O atoms while carrying opposite effective charges.

By analogy with the polarizability, we define  $Z_i$  and  $C_i$  values for each SU such that

$$\bar{Z}^2 = \sum_i x_i Z_i^2, \quad \text{and} \quad \bar{C}^{-1} = \sum_i x_i C_i^{-1}, \quad (4)$$

though the locality and the additivity of these parameters is not guaranteed *a priori*. We determine the optimal values  $Z_i$  and  $C_i$  in the same way as for  $\alpha_i$  (Table II). In Fig. 2(a), we compare the values of  $\Delta\epsilon$  obtained using Eqs. (3) and (4) with those calculated from first principles.

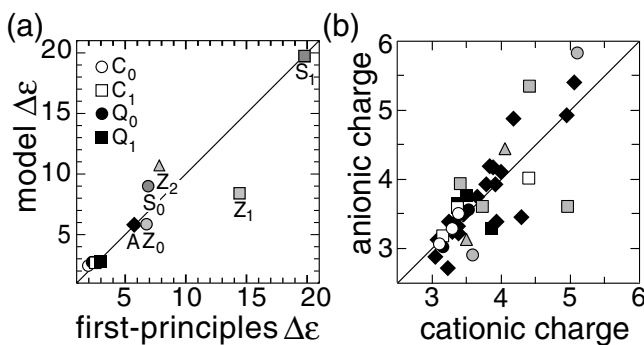


FIG. 2. (a) Comparison between  $\Delta\epsilon$  derived within our model scheme [Eqs. (3) and (4)] and calculated from first principles. (b) Anionic vs cationic charge (see text). Same symbols as in Fig. 1.

For the nine crystalline models, the agreement between the two sets of data is quite good, though not as impressive as for  $\epsilon_\infty$ . Differences result primarily from the determination of  $\bar{C}$ , which gives an average error of 18%. This error is severely affected by the singular case of  $Z_1$  (see below). By contrast, the values of  $\bar{Z}$  given by Eq. (4) agree very well with those computed from first principles, showing an average and maximal error smaller than 2% and 3%, respectively. *A posteriori*,  $\bar{C}$  appears to be less local and additive than  $\bar{Z}$ .

In fact, the locality of  $\bar{C}$  is closely related to the dynamical charge neutrality of the SUs. The most important contributions to  $\bar{C}$  arise from infrared active modes of low frequency. To the extent that the dynamical charge carried by the SUs vanishes, long-range vibrations in which the SUs move as rigid units will be infrared inactive and the dominating contributions to  $\bar{C}$  will come from rather localized distortive vibrations. Therefore, the closer the SUs are from dynamical charge neutrality, the more local  $\bar{C}$ , and the more valid our scheme. In Fig. 2(b), we report, for every SU in our set of models, the anionic charge [14] versus the cationic charge. Dynamical charge neutrality is observed for most of the SUs. Note that the case of  $Z_1$ , which presents the largest discrepancy in  $\bar{C}$ , is also the one for which charge neutrality is the least well satisfied. Our scheme should be more accurate for disordered systems, where the localization of vibrational modes is enhanced and the dynamical charge neutrality appears better respected (see Fig. 2(b) and Ref. [15]). In fact, for the amorphous model, which was not used to determine the  $Z_i$  and  $C_i$  values, the agreement between the model and the first principles  $\Delta\epsilon$  is excellent with an error smaller than 1% [see Fig. 2(a)].

For Zr silicates of known composition in terms of SUs, the parameters in Table II fully determine the dielectric constants. Several points are noteworthy. First, the three parameters of Zr-centered SUs all contribute to enhancing the dielectric constants over those of Si-centered ones of corresponding coordination [16]. This is clearly at the origin of the increase of  $\epsilon_\infty$  and  $\epsilon_0$  with increasing Zr concentration. Second, while the polarizability  $\alpha_i$  of a given SU (Si- or Zr-centered) steadily decreases with increasing coordination, such a regular behavior is not observed for the parameters  $Z_i$  and  $C_i$  determining  $\Delta\epsilon$ . In fact,  $Z_i$  and  $C_i$  concurrently vary to enhance the contribution of  $\text{ZrO}_6$  units, which are the SUs giving the largest contribution to  $\Delta\epsilon$  in amorphous Zr silicates.

Based on the scheme given by Eqs. (1)–(4), we can now estimate  $\epsilon_\infty$  and  $\epsilon_0$  for amorphous  $(\text{ZrO}_2)_x(\text{SiO}_2)_{1-x}$  as a function of Zr composition ( $0 < x < 0.5$ ). Using measured densities for Zr silicates [9], we first obtain  $\epsilon_\infty$  as a function of  $x$ . As shown in Fig. 3, our theoretical values [20] are in excellent agreement with available experimental data [8,9].

To apply our scheme for  $\Delta\epsilon$ , we need additional information on the cationic coordination. We take the Si

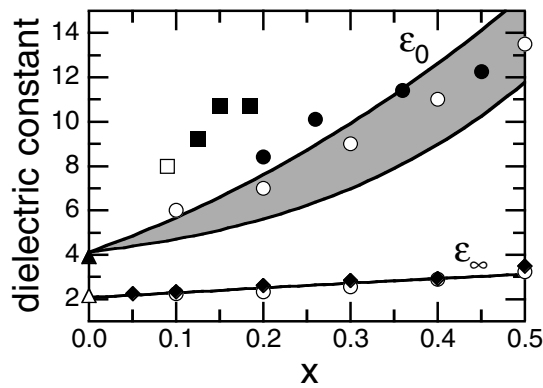


FIG. 3. Dielectric constants ( $\epsilon_\infty$  and  $\epsilon_0$ ) as a function of composition  $x$  for amorphous  $(\text{ZrO}_2)_x(\text{SiO}_2)_{1-x}$ . The gray region corresponds to results derived from our model scheme and reflects the indetermination of the number of  $\text{ZrO}_6$  units. The upper curve delimiting the band corresponds to structures entirely composed of  $\text{ZrO}_6$  units, while the lower curve represents a smooth transition from a structure composed of  $\text{ZrO}_4$  units at  $x = 0$  to one composed of  $\text{ZrO}_8$  units at  $x = 0.5$ , without the occurrence of any  $\text{ZrO}_6$  unit. Experiment: Ref. [9] (black diamonds), Ref. [7] (black circles), Ref. [8] (white circles), Ref. [4] (black squares), Ref. [17] (white squares), Ref. [18] (black triangles), and Ref. [19] (white triangles).

atoms to be fourfold coordinated. The coordination of Zr atoms is less well determined. Recent EXAFS measurements [5] indicate that the average Zr coordination grows from about four to about eight for Zr concentrations increasing from  $x \sim 0$  to  $x \sim 0.5$ . In Fig. 3, we report calculated  $\epsilon_0$  for amorphous  $(\text{ZrO}_2)_x(\text{SiO}_2)_{1-x}$  as a function of  $x$ , together with the available experimental data [4,7,8,17]. The theoretical results are given in the form of a band reflecting the indetermination of the coordination of Zr atoms. We modeled the dielectric constant in terms of suitable distributions of three representative structural units ( $\text{ZrO}_4$ ,  $\text{ZrO}_6$ , and  $\text{ZrO}_8$ ). The upper curve delimiting the band in Fig. 3 corresponds to structures entirely composed of  $\text{ZrO}_6$  units. The lower curve is for amorphous systems which do not contain any  $\text{ZrO}_6$  units. The average Zr coordination varies linearly from four to eight between  $x = 0$  and  $x = 0.5$ , with concentrations of  $\text{ZrO}_4$  and  $\text{ZrO}_8$  SUs varying at most quadratically. Note that the upper part of the band agrees well with the recent experimental data of Refs. [7,8]. The earlier data (Refs. [4,17]) cannot be explained by our theory, not even for amorphous Zr silicates exclusively composed of  $\text{ZrO}_6$  units. Figure 3 shows that, for a sufficient amount of  $\text{ZrO}_6$  units, values of  $\epsilon_0$  at intermediate  $x$  can indeed be larger than estimated from a linear interpolation between  $\text{SiO}_2$  and  $\text{ZrSiO}_4$ . However, in accord with recent experiments [7,8], our theory indicates that the extent of this effect is more limited than previously assumed [4,5].

In summary, we have provided a simple scheme which relates the optical and static dielectric constants of Zr silicates to their underlying structure. Our theory sup-

ports recent experiments which find a close to linear dependence of  $\epsilon_0$  on the Zr fraction  $x$ , and shows that higher dielectric constants can be achieved by increasing the concentration of  $\text{ZrO}_6$  structural units. The scheme presented here can be applied to other amorphous systems composed of SUs (e.g., oxide glasses), provided the dynamical charge neutrality is locally satisfied.

We thank R. B. van Dover for providing Ref. [8] prior to publication. Support is acknowledged from the FNRS-Belgium (G.-M. R. and X. G.), the FRIA-Belgium (F. D.), the Swiss FNS under Grants No. 21-55450.98 and No. 620-57850.99 (A. B. and A. P.), the FRFC project (No. 2.4556.99), the Belgian PAI-5/1/1, and the Swiss Center for Scientific Computing.

- [1] M. Schulz, *Nature (London)* **399**, 729 (1999).
- [2] D. A. Muller *et al.*, *Nature (London)* **399**, 758 (1999).
- [3] G. D. Wilk, R. M. Wallace, and J. M. Anthony, *J. Appl. Phys.* **89**, 5243 (2001).
- [4] G. D. Wilk and R. M. Wallace, *Appl. Phys. Lett.* **76**, 112 (2000); G. D. Wilk, R. M. Wallace, and J. M. Anthony, *J. Appl. Phys.* **87**, 484 (2000).
- [5] G. Lucovsky and G. B. Rayner, Jr., *Appl. Phys. Lett.* **77**, 2912 (2000).
- [6] H. A. Kurtz and R. A. B. Devine, *Appl. Phys. Lett.* **79**, 2342 (2001).
- [7] W.-J. Qi *et al.*, *Appl. Phys. Lett.* **77**, 1704 (2000).
- [8] R. B. van Dover, L. Manchanda, M. L. Green, G. Wilk, E. Garfunkel, and B. Busch (to be published).
- [9] M. Nogami, *J. Non-Cryst. Solids* **69**, 415 (1985).
- [10] J.-P. Crocombette and D. Ghaleb, *J. Nucl. Mater.* **257**, 282 (1998).
- [11] ABINIT is a common project of the Université Catholique de Louvain, Corning Incorporated, and other contributors (<http://www.ABINIT.org>).
- [12] G.-M. Rignanese, X. Gonze, and A. Pasquarello, *Phys. Rev. B* **63**, 104305 (2001).
- [13] Orientational averages are given.
- [14] The anionic charge of a SU is defined as the sum of the effective charges of its O atoms weighted by the inverse of the number of SUs to which the O atom belongs.
- [15] A. Pasquarello and R. Car, *Phys. Rev. Lett.* **79**, 1766 (1997).
- [16] In Table II, the value of  $C$  for  $\text{SiO}_4$  apparently leads to a higher contribution to  $\Delta\epsilon$  than that for  $\text{ZrO}_4$ . This is an artifact of our approach to determine the  $Z_i$  and  $C_i$ . Indeed, in Fig. 1, the  $\text{Si} \rightarrow \text{Zr}$  substitution for  $C_0$  or  $Q_0$  clearly leads to a decrease of  $\bar{C}$ .
- [17] V. Misra, from Ref. [5] (unpublished).
- [18] Arun K. Varshneya, *Fundamental of Inorganic Glasses* (Academic Press Inc., San Diego, CA, 1994), p. 364.
- [19] *Handbook of Chemistry and Physics*, edited by Robert C. Weast (The Chemical Rubber Co., Cleveland, OH, 1972), 52nd ed., p. E-204.
- [20] Because the various Zr-centered units have close  $\alpha$  values compared to  $\text{SiO}_4$  (Table II), the effect of Zr coordination on  $\epsilon_\infty$  is negligible.